J Fluoresc (2013) 23:1313–1318
DOI 10.1007/s10895-013-1265-z

ORIGINAL PAPER

Synthesis of Fluorescent Gold Nanoclusters Directed by Bovine Serum Albumin and Application for Nitrite Detection

Qiaoli Yue · Lijun Sun · Tongfei Shen · Xiaohong Gu · Shuqiu Zhang · Jifeng Liu

Received: 1 April 2013 / Accepted: 1 July 2013 / Published online: 13 July 2013

Abstract In the present work, gold nanocluster (GNC) induced by bovine serum albumin (BSA) was synthesized as a novel fluorescence probe to detect nitrite (NO_2^-) sensitively and selectively. The fluorescence of GNC was found to be quenched effectively by NO_2^-. Under the optimum conditions, it was found that the change of fluorescence intensity was proportional with the concentration of NO_2^- in the linear range of 0.1–50 μM (R=0.9990), with a detection limit (S/N=3) of 30 nM. The absorption spectroscopy, circular dichroism (CD), and X-ray photoelectron spectroscopy (XPS) studies were employed to discuss the quenching mechanism. In addition, the present approach was successfully applied in real water samples.

Keywords Nitrite · Gold nanocluster · Bovine serum albumin · Water samples

Introduction

Nitrite (NO_2^-) is present at trace levels in soil, natural waters, and plant and animal tissues [1]. In surface waters, NO_2^- is generally present in low concentrations. Their presence in ground water is less common. In waste water NO_2^- frequently occurs, even in fairly high concentrations. A principal concern about NO_2^- is the formation of carcinogenic nitrosamines in meats containing NO_2^- when meat is charred or overcooked. Such carcinogenic nitrosamines can be formed from the reaction of NO_2^- with secondary amines under acidic conditions (such as occurs in the human stomach) as well as during the curing process used to preserve meats [2].

Therefore, the determination of NO_2^- in water, food, and environmental matrices is of vital significance. In recent years, trace NO_2^- determination has attracted great interests. The methods including chromatography [3, 4], capillary electrophoresis [5], electrometry [6–9], chemiluminescence [10], spectrophotometry [11, 12], electron spin resonance, diffuse reflectance spectroscopy [13], spectrofluorimetry [14, 15], and other method [16]. Among all of the methods, sepectrofluorimetry is widely used to its simplicity, sensitivity, excellent limits of detection obtained, and low-cost [17].

Recently, the advances in noble metal clusters open a promising field toward the development of a satisfying fluorescence probe. The noble metal clusters possess particularly small size (typically consist of 2–20 atoms), exhibit a strong fluorescence emission and excellent photostability [18–20]. For their synthesis, bovine serum albumin (BSA) can serve as an effective stabilizing agents due to its amine, carboxyl, and thiol groups in the structure. For instance, BSA-directed fluorescent gold clusters have been successfully used as fluorescent probes for Hg^{2+} and Cu^{2+} ions sensing [21, 22]. Inspired by the protein-directed inorganic nanomaterial synthesis [21, 22], we hypothesize that denatured BSA (dBSA) can provide the scaffolds necessary to interact with and sequester the inorganic ions during the formation of metal clusters. Herein, we synthesized gold nanoclusters (GNCs) directed and stabilized by BSA and developed as a fluorescent probe for the application of NO_2^- detection. It is found that the fluorescence of BSA-GNCs can sensitively respond

Q. Yue · L. Sun · T. Shen · J. Liu (✉)
Department of Chemistry, Liaocheng University,
Liaocheng 252059, People's Republic of China
e-mail: liujifeng111@gmail.com

X. Gu · S. Zhang
Shandong Provincial Key Lab of Test Technology on Food Quality and Safety, Shandong Academy of Agricultural Sciences,
Jinan 250100, China

toward the concentration of NO_2^-. Therefore, a sensitive and cost-effective fluorescent sensor for the determination of NO_2^- was fabricated.

Experimental Section

Materials

Tetrachloroauric acid trihydrate ($HAuCl_4 \cdot 3H_2O$) (99.9+%), tris (hydroxymethyl)-aminomethane (Tris), bovine serum albumin (BSA), the membrane dialysis bag (molecular weight cutoff 12 kDa), guanidine hydrochloride and sodium borohydride ($NaBH_4$) were purchased from Sigma-Aldrich Chemical Co. (St. Louis, MO). NaCl, Na_2HPO_4, NaH_2PO_4 and other common chemicals used were obtained from Beijing Chemical Works (Beijing, China). All reagents were used as obtained without further purification until and unless stated. Deionized water (≥ 18.2 MΩ) prepared by a Millipore water system was used throughout the experiments.

Apparatus

Absorption spectra of GNCs were collected using a Lambda 25 UV–vis spectrometer (Perkin Elmer, USA). Fluorescence measurements were performed on an F-7000 spectrophotometer (Hitachi, Japan) with a common 2 mm slit sample cell. Transmission Electron Microscopy (TEM) images of GNCs were obtained on a JEM 2100 (JEOL, Japan) TEM with 120 kV acceleration voltage. Circular dichroism (CD) experiments were performed at room temperature using a J-810-150S CD spectropolarimeter (JASCO, Japan). Each measurement was the average of five repeated scans recorded from 220 to 320 nm in a 1 cm-path length quartz cell at a scanning rate of 50 nm/min. X-ray photoelectron spectroscopy (XPS) measurements were carried out on an ESCALAB-MKII spectrometer (VG Co., U.K.) with Al Kα X-ray radiation as the X-ray source for excitation.

Synthesis of dBSA Coated GNCs

dBSA was prepared according to a reported method with some modifications [21]. Native BSA solution (30 ml, 50 mg/ml) was mixed with guanidine hydrochloride solution (20 ml, 6 M) and incubated for 60 min in an ice-bath, and the excess saline (i.e., guanidine and chloride ion) in dBSA was removed by washing with water and centrifugation. The final concentration of the dBSA was adjusted to ~50 mg/ml.

The dBSA directed approach was employed to synthesize GNCs similar with the earlier [20]. $HAuCl_4$ solution (20 mM, 20 ml) was incubated with the dBSA solution (40 ml, 50 mg/ml) for 1 h in an ice-bath, then $NaBH_4$ (40 mM, 20 ml) was added, and the mixture was incubated overnight at 4 °C. The dBSA coated GNCs were obtained by further purification via centrifugation. The absorption and emission spectra, TEM images of GNCs were tested. The final solution was stored at 4 °C when not in use.

Fluorescence Experiments for NO_2^- Detection

A typical NO_2^- detection procedure was conducted as follows. NO_2^- solution at different concentrations was obtained by serial dilution of the stock solution. The concentration of as-prepared GNCs was calculated of 5.0 mg ml^{-1} by lyophilization. 0.5 mg ml^{-1} GNCs was used for NO_2^- detection. Typically, 50 μl of NO_2^- solutions with various concentrations were mixed with 5 μl of the as-prepared GNCs solution. After mixing for about 10 min, 545 μl of water was added to bring the final volume to 600 μl for fluorescence spectra measurements at room temperature.

To evaluate the selectivity of NO_2^- fluorescence detection by using dBSA coated GNCs, metal ions and other cations such as Ca^{2+}, Cd^{2+}, Co^{2+}, Cu^{2+}, Mg^{2+}, Zn^{2+}, Fe^{2+}, Ni^{2+}, Cr^{3+}, Al^{3+}, Ba^{2+}, Cd^{2+}, NO_3^-, PO_4^{3-}, SO_4^{2-}, CO_3^{2-}, HCO_3^{2-}, HPO_4^{2-}, HSO_3^-, $H_2PO_4^-$, Cl^-, F^-, Br^- and NH_4^+ were also tested and the response recorded and analyzed.

Results and Discussion

Characterization of the dBSA-GNCs

In this study, BSA was chosen as the model protein because it is widely used and commercially available and has proven to work in the synthesis of fluorescent GNCs [21, 23]. BSA consists of 35 potential thiol groups as noted earlier, due to the 17 disulfide bonds and 1 free cysteine. In this case, if these 35 cysteine residues could be completely liberated, they could act as chelating groups for sequestering Au^{3+} and as polyvalent ligands for passivating the surface of GNCs. The dBSA with 35 liberated cystein residues was obtained by treating native BSA with guanidine as described in Experimental Section. And then dBSA-GNCs were prepared by first sequestering Au^{3+} with dBSA and reducing Au^{3+} to Au^0 clusters with $NaBH_4$. To confirm the formation of the dBSA-GNCs, TEM images were obtained. As shown in Fig. 1, the as prepared GNCs were approximately spherical in shape and about 1.3 nm in diameter.

Spectral Characteristics of BSA-GNCs

BSA-stabilized GNCs (BSA-GNCs) as-prepared showed dark brown under daylight lamp, and emitted an intense red fluorescence in UV light (365 nm) (Fig. 2). The character of the spectra was consistent with the literature [18], which suggested the successful preparation of BSA-stabilized

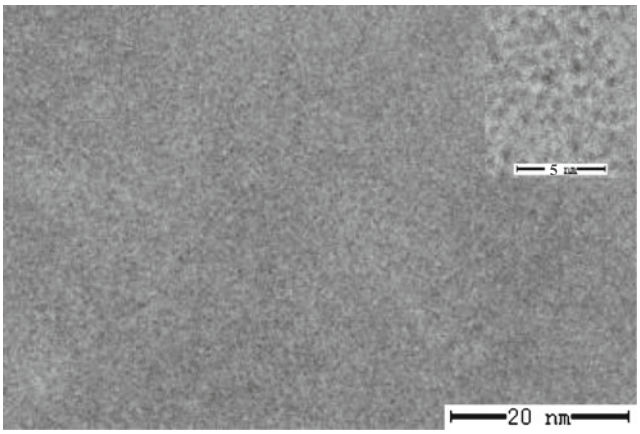

Fig. 1 TEM images of GNCs using BSA for surface protection, the enlarged particles are seen in the inset

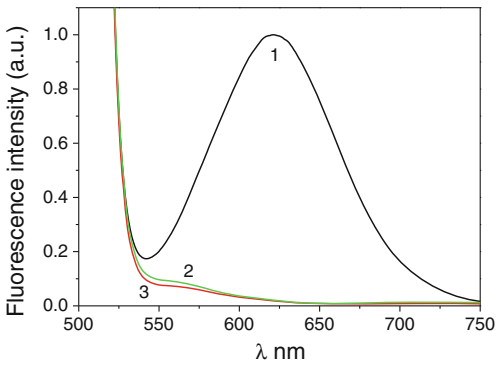

Fig. 3 Fluorescence spectra of the GNCs stabilized by dBSA (1), oxidized dBSA (2), and reduced dBSA (3), respectively

fluorescent GNCs. From Fig. 2a, it can be shown that the typical excitation and emission spectra of BSA-GNCs in aqueous solution, in which the emission spectrum of BSA-GNCs displayed a peak around 622 nm upon excitation of 502 nm, respectively. Moreover, under the UV lamp only red fluorescence was obtained. And then the red fluorescence of BSA-GNCs was used. It was reported that the red emission was considered to arise from intraband transitions of free electrons of the GNCs [24]. The fluorescence response of BSA-GNCs to NO_2^- was firstly investigated.

To exclude the possibility that the observed fluorescence was from oxidized or reduced protein cage, the following experiments were carried out. Firstly, oxidized dBSA was prepared by reacting dBSA with Ce^{4+}, and reduced dBSA was obtained by reacting dBSA with $NaBH_4$, respectively. Fluorescent emission of the products was then measured. As illustrated in Fig. 3, none of these products gave fluorescence emission, which confirmed the fluorescence of GNCs.

Detection of NO_2^- Based on Fluorescent BSA-GNCs

The biosensor response usually can be affected by the solution pH, performance temperature, and the reaction times. Thereafter, to achieve the sensitive detection of NO_2^- under optimum conditions, the effects of these parameters were studied. The response was independently tested thrice for each pH, temperature, and an average value was calculated. Results showed that the fluorescence response toward NO_2^- changed slightly when pH of GNCs solution varied from 5 to 9, or the temperature varied in the range of 15–45 °C (Fig. 4). However, considering the sensor for easy control, pH 6.0 and room temperature 25 °C were chosen as the experimental conditions. Moreover, the effect of incubation time on the response was also investigated. It can be indicated from the result that the reaction could reach equilibrium within 5 min.

Figure 5a depicted the typical fluorescence response of the dBSA-GNCs in the presence of different concentration of NO_2^-. After the addition of NO_2^-, the fluorescence intensity of dBSA-GNCs decreased gradually. Meanwhile, a discernible change in the maximum of the emission spectrum accompanied with quenching. The quenching efficient for relative fluorescence intensity (F_0/F-1, where F and F_0 were the fluorescent intensity in the presence and absence of NO_2^-, respectively) *vs*. the NO_2^- concentration ($[NO_2^-]$), i.e. Stern-Volmer quenching relationship, was plotted in Fig. 5b. The fluorescence response of GNCs toward NO_2^- proved to be very sensitive. The resulting calibration curve was linear over the range from 0.1 μM to 50 μM with the correlation coefficient of 0.9990. The detection limit was as low as 30 nM (S/N=3). The relative standard deviation (RSD)

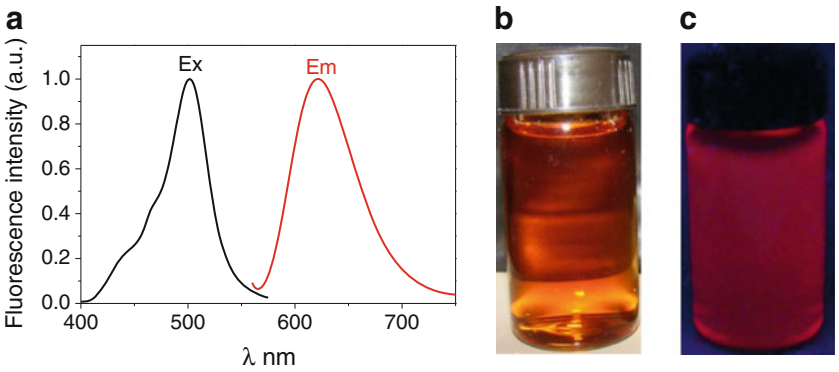

Fig. 2 Excitation and emission spectrum with the peaks at 502 nm and 622 nm, respectively (**a**) and the photographs of GNCs in daylight (**b**) and UV lamp (**c**)

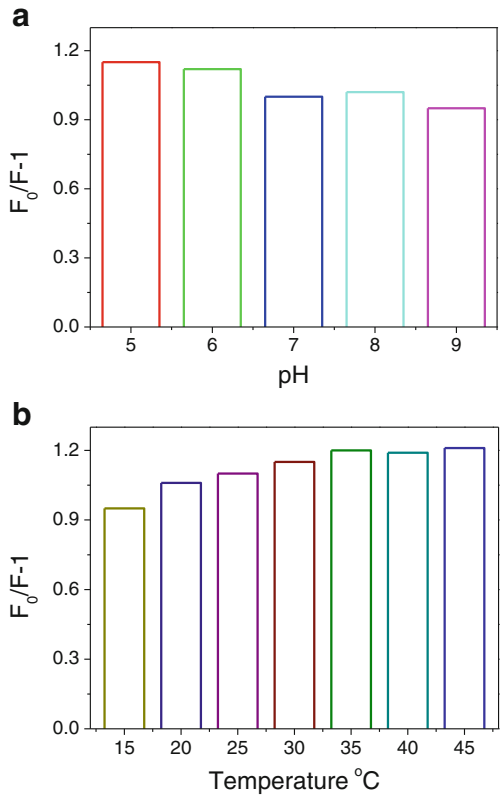

Fig. 4 Dependence of the fluorescence response (F_0/F-1) toward 20 μM NO_2^- with GNCs on the pH of the buffer (**a**), the temperature of the system (**b**) (F_0 and F are the fluorescence intensity in the absence and presence of NO_2^-, respectively). The *data* showed the average of three separate measurements

was no more than 3.1 % obtained for five replicate detections of 0.1, 0.5 and 1.0 μM NO_2^-, which indicated a good reproducibility of the present method.

Selectivity of the Biosensor for NO_2^- Detection

Under optimum conditions, the selectivity was determined by test fluorescence signal changes of GNCs that occurred within 5 min after separately adding various other substances as described in Experimental Section. The tolerance limit of the substances for the determination of 1.0 μM NO_2^- was listed in Table 1. The results showed no interference with the detection of NO_2^-. An excellent selectivity for NO_2^- over common anions (all sodium salts) and cations was achieved using the proposed sensing technique.

Mechanism of NO_2^- Induced Quenching of Fluorescence of dBSA-GNCs

The mechanism of the sensitive fluorescence response of GNCs toward NO_2^- has been also investigated. Considering the structure of the GNCs, thiol group of cysteine residues in dBSA played an important role as the stabilizer for GNCs. Herein, it was presumed that the quenching effect of the system fluorescence might be attributed to the specific interactions between NO_2^- the amino acids present in the dBSA chain and leading to the damage of GNCs structure.

Disulfides and sulfonates were not chemisorbed, and therefore, can be easily removed from the GNCs surface [18]. Thus, these reactions could lead to a rapid deterioration of structure of GNCs and quenching the fluorescence effectively. To verify the assumption, the following experiments were then performed. Firstly, the absorption spectra of BSA were recorded in presence and absence of NO_2^-. As shown in Fig. 6a, BSA solution exhibited a characteristic absorbance at 278 nm, which mainly originates from aromatic residues and disulfide bonds. In the presence of 10 mM NO_2^-, the peak position shifted distinctly, which might be assigned to the specific interaction of NO_2^- and BSA. Furthermore, CD spectra of BSA in the presence and absence of NO_2^- were drawn (Fig. 6b), which was widely used in elucidating the secondary structure of proteins. The previous report showed that the formation of GNCs did not affect the conformations of the protein [21]. Therefore, BSA rather than dBSA-GNCs was tested. The measurements were done at nearly neutral pH and samples prepared in PBS and later diluted with deionized water. The concentration of BSA and $NaNO_2$ were 10 μM and 50 μM, respectively. The BSA molecule mainly existed in an α-helical structure and showed a positive CD at 192 nm and two negative CD at 208 nm and 222 nm, respectively. In the presence of $NaNO_2$

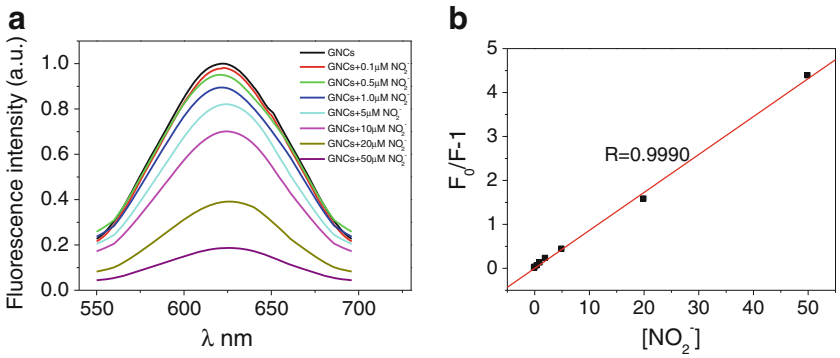

Fig. 5 Quenching effect of NO_2^- on the fluorescence spectra of GNCs (**a**) and the Stern-Volmer curve of GNCs-NO_2^- system (**b**). The *data* showed the average of three separate measurements

Table 1 Tolerance limit of various substances on the determination of 1.0 μM NO_2^-

Tolerance	Substances
1000	Ca^{2+}, NO_3^-, PO_4^{3-}, SO_4^{2-}, CO_3^{2-}, HCO_3^{2-}, HPO_4^{2-}, HSO_3^-, $H_2PO_4^-$, Cl^-, F^-, Br^-, NH_4^+
500	Cd^{2+}, Co^{2+}, Cu^{2+}, Mg^{2+}, Ni^{2+}, Ba^{2+}
200	Fe^{2+}, Zn^{2+}, Al^{3+}
100	Cu^{2+}, Cr^{3+}

the CD spectrum showed an obvious change for peak intensity and a slight red shift, which suggested the effect of NO_2^- on the protein. Secondly, XPS data indicated that GNCs might be oxidized during the reaction, as shown in Fig. 6c. For GNCs, Au $4f_{7/2}$ showed a peak at 83.1 eV, which was in agreement with the reference value [25]. In the presence of NO_2^-, Au $4f_{7/2}$'s peak shifted to 84.2 eV, which corresponds to Au oxidation states [26, 27]. XPS results clearly indicated that Au oxidation took place during the reaction of NO_2^- and BSA. Furthermore, the lifetime for the excited state of the

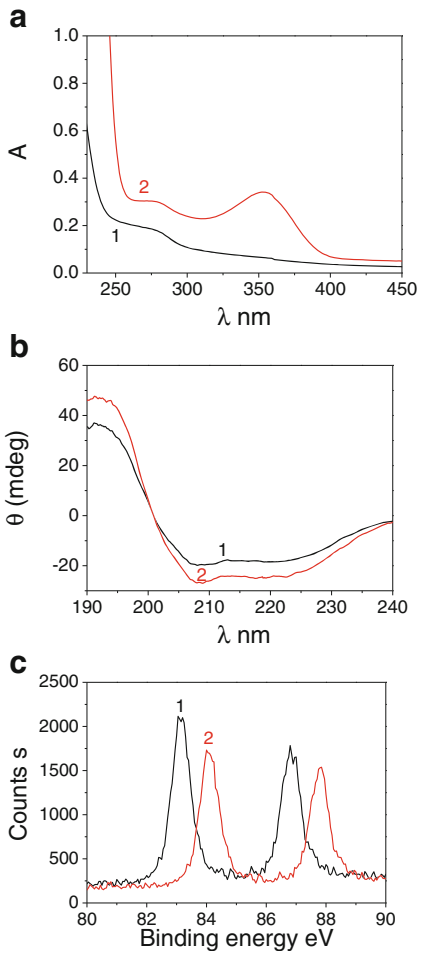

Fig. 6 Absorption (**a**) and CD spectra of BSA (**b**) and XPS of GNCs (**c**) in the absence (curve 1) and presence (curve 2) of NO_2^-

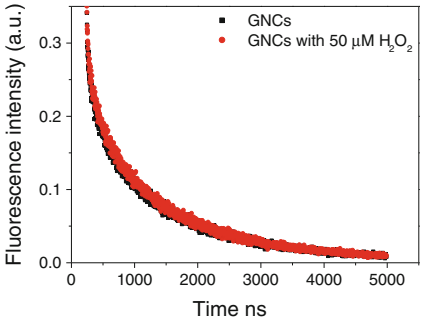

Fig. 7 Fluorescence decay of the GNCs as a function of time in the presence of 50 μM H_2O_2

GNCs before and after addition of NO_2^- was also compared (1.332±0.031 μs and 1.361±0.028 μs, respectively, Fig. 7). It can be found that no obvious change was observed with the addition of NO_2^- to the lifetime of GNCs. The results indicated that the fluorescence quenching induced by NO_2^- was mainly the static quenching mode, and which accorded with the fact that the structure destruction of GNCs leading to the quenching of the fluorescence [28].

Determination of NO_2^- in Real Samples

To investigate the feasibility of the biosensor for NO_2^- detection in real samples including tap water, river water and lake water samples were analyzed. River water and lake water samples were obtained from Tuhai River in Liaocheng and the lake in the campus of Liaocheng University, respectively. The samples collected were first filtered through a 0.22 μm membrane, then centrifuged for 10 min at 10 000 rpm and detected according to the general procedure with three replicates. The results averaged from three determinations are summarized in Table 2.

The present assay displays a high selectivity for NO_2^- against a background of competing analytes. Moreover, the results show a good agreement with that determined by the standard spectrophotometric method, and the recoveries for the samples were 96–105 %.

Table 2 Determination of NO_2^- in water samples[a]

Sample	Proposed method/μM	Standard method/μM	Added/ μM	Found/ μM	Recovery (%)
Tap water	0.29	0.26	0.50	0.51	102
			1.0	0.98	98
River water	0.45	0.47	0.5	0.49	98
			1.0	1.05	105
Lake water	0.52	0.54	0.5	0.48	96
			1.0	0.99	99

[a] Mean of three separated measurements

Conclusions

In summary, it was developed a new and facile method for sensitive detection of NO_2^- based on a biomacromolecule-stabilized GNCs. The detection mechanism was based on the specific interaction between NO_2^- and BSA leading to the structural damage of GNCs and fluorescence decrease. The fluorescence of GNCs enabled the assay of NO_2^- in the range of 0.1–50 μM with a detection limit of 30 nM, which was lower than that of prior report [29]. By comparison, the present sensor for NO_2^- detection showed many advantages including requiring no complicated preparation procedure and use only commercially available materials over previous approaches. It also exhibited environmentally friendly feature and good sensitivity. Moreover, the present biosensor possessed red emission and excellent biocompatibility, which presage more opportunities for studying environmental real samples in the future.

Acknowledgments Q. Yue and J. Liu thank Natural Science Foundation of China for Funding (21005036, 20875042, 21075058, 21127006). This work was also supported by Natural Science Foundation (ZR2010BZ004, JQ201106), Research Fund of Shandong Academy of Agricultural Sciences and Doctoral Fund of Liaocheng University.

References

1. Butler AR, Feelisch M (2008) Therapeutic uses of inorganic nitrite and nitrate: from the past to the future. Circulation 117:2151
2. Masuda M, Mower HF, Pignatelli B, Celan I, Friesen MD, Nishino H, Ohshima H (2000) Formation of N-nitrosamines and N-nitramines by the reaction of secondary amines with peroxynitrite and other reactive nitrogen species: comparison with nitrotyrosine formation. Chem Res Toxicol 13:301
3. Li YT, Whitaker JS, McCarty CL (2011) Reversed-phase liquid chromatography/electrospray ionization/mass spectrometry with isotope dilution for the analysis of nitrate and nitrite in water. J Chromatogr A 1218:476
4. He LJ, Zhang KG, Wang CJ, Luo XL, Zhang SS (2011) Effective indirect enrichment and determination of nitrite ion in water and biological samples using ionic liquid-dispersive liquid–liquid microextraction combined with high-performance liquid chromatography. J Chromatogr A 1218:3595
5. Wang X, Adams E, Schepdael AV (2012) A fast and sensitive method for the determination of nitrite in human plasma by capillary electrophoresis with fluorescence detection. Talanta 97:142
6. Zhang W, Yuan R, Chai YQ, Zhang Y, Chen SH (2012) A simple strategy based on lanthanum-multiwalled carbon nanotube nanocomposites for simultaneous determination of ascorbic acid, dopamine, uric acid and nitrite. Sens Actuators B 166–167:601
7. Wang J, Diao P, Zhang Q (2012) Dual detection strategy for electrochemical analysis of glucose and nitrite using a partitionally modified electrode. Analyst 137:145
8. Muchindu M, Waryo T, Arotiba O, Kazimierska E, Morrin A, Killard AJ, Smyth MR, Jahed N, Kgarebe B, Baker PGL, Iwuoha EI (2010) Electrochemical nitrite nanosensor developed with amine- and sulphate-functionalised polystyrene latex beads self-assembled on polyaniline. Electrochim Acta 55:4274
9. Miao P, Shen M, Ning LM, Chen GF, Yin YM (2011) Functionalization of platinum nanoparticles for electrochemical detection of nitrite. Anal Bioanal Chem 399:2407
10. Li JG, Li QQ, Lu C, Zhao LX (2011) Determination of nitrite in tap waters based on fluorosurfactant-capped gold nanoparticles-enhanced chemiluminescence from carbonate and peroxynitrous acid. Analyst 136:2379
11. Pourreza N, Fathi MR, Hatami A (2012) Indirect cloud point extraction and spectrophotometric determination of nitrite in water and meat products. Microchem J 104:22
12. Daniel WL, Han MS, Lee J-S, Mirkin CA (2009) Colorimetric nitrite and nitrate detection with gold nanoparticle probes and kinetic end points. J Am Chem Soc 131:6362
13. Luiz VHM, Pezza L, Pezza HR (2012) Determination of nitrite in meat products and water using dapsone with combined spot test/diffuse reflectance on filter paper. Food Chem 134:2546
14. Wang LL, Li B, Zhang LM, Zhang LG, Zhao HF (2012) Fabrication and characterization of a fluorescent sensor based on Rh 6G-functionlized silica nanoparticles for nitrite ion detection. Sens Actuators B 171–172:946
15. Xue ZW, Wu ZS, Han SF (2012) A selective fluorogenic sensor for visual detection of nitrite. Anal Methods 4:2021
16. Xiong Y, Zhu DQ, Duan CF, Wang JW, Guan YF (2010) Small-volume fiber-optic evanescent-wave absorption sensor for nitrite determination. Anal Bioanal Chem 396:943
17. Gao F, Zhang L, Wang L, She SK, Zhu CQ (2005) Ultrasensitive and selective determination of trace amounts of nitrite ion with a novel fluorescence probe mono[6-N(2-carboxy-phenyl)]-β-cyclodextrin. Anal Chim Acta 533:25
18. Jin LH, Shang L, Guo SJ, Fang YX, Wen D, Wang L, Yin JY, Dong SJ (2011) Biomolecule-stabilized Au nanoclusters as a fluorescence probe for sensitive detection of glucose. Biosens Bioelectron 26:1965
19. Lin C-AJ, Yang T-Y, Lee C-H, Huang SH, Sperling RA, Zanella M, Li JK, Shen J-L, Wang H-H, Yeh H-I, Parak WJ, Chang WH (2009) Synthesis, characterization, and bioconjugation of fluorescent gold nanoclusters toward biological labeling applications. ACS Nano 3:395
20. Guo CL, Irudayaraj J (2011) Fluorescent Ag clusters via a protein-directed approach as a Hg(II) ion sensor. Anal Chem 83:2883
21. Xie JP, Zheng YG, Ying JY (2009) Protein-directed synthesis of highly fluorescent gold nanoclusters. J Am Chem Soc 131:888
22. Xie JP, Zheng YG, Ying JY (2010) Highly selective and ultrasensitive detection of Hg^{2+} based on fluorescence quenching of Au nanoclusters by Hg^{2+}–Au^{+} interactions. Chem Commun 46:961
23. Durgadas CV, Sharmaa CP, Sreenivasan K (2011) Fluorescent gold clusters as nanosensors for copper ions in live cells. Analyst 136:933
24. Zheng J, Nicovich PR, Dickson RM (2007) Highly fluorescent noble-metal quantum dots. Annu Rev Phys Chem 58:40
25. Brust M, Walker M, Bethell D, Schiffrin DJ, Whyman R (1994) Synthesis of thiol-derivatised gold nanoparticles in a two-phase Liquid-Liquid system. J Chem Soc Chem Commun 801
26. Dasog M, Scott RWJ (2007) Understanding the oxidative stability of gold monolayer-protected clusters in the presence of halide ions under ambient conditions. Langmuir 23:3381
27. Hostetler MJ, Wingate JE, Zhong CJ, Harris JE, Vachet RW, Clark MR, Londono JD, Green SJ, Stokes JJ, Wignall GD, Glish GL, Porter MD, Evans ND, Murray RW (1998) Alkanethiolate gold cluster molecules with core diameters from 1.5 to 5.2 nm: core and monolayer properties as a function of core size. Langmuir 14:17
28. Valeur B (2001) Molecular fluorescence: principles and applications. Wiley-VCH, Germany
29. Zhang T, Fan HL, Jin QH (2010) Sensitive and selective detection of nitrite ion based on fluorescence superquenching of conjugated polyelectrolyte. Talanta 81:95